

RSC Sustainability

rsc.li/rsccsus



ISSN 2753-8125

PAPER

Rodrigo O. M. A. de Souza *et al.*
Chemo-enzymatic cascades for the sustainable
transformation of canola oil into hydrocarbon fuels



Cite this: *RSC Sustainability*, 2025, **3**, 3407

Chemo-enzymatic cascades for the sustainable transformation of canola oil into hydrocarbon fuels[†]

Lucas B. Barbosa,^a Caio M. Pacheco, ^a Isabela G. da Silva,^a Mauro R. B. P. Gomez,^a Alexandre S. França,^a Gabriela C. Breda,^a Matheus C. Silva,^a Patrícia S. de Alencar,^a Fernanda A. Lima,^a Raquel A. C. Leão,^a Rodrigo V. Almeida^b and Rodrigo O. M. A. de Souza ^{a*}

This study introduces a novel chemo-enzymatic cascade methodology for the sustainable conversion of canola oil into fuel-like hydrocarbons, combining biocatalysis and continuous-flow technology. The proposed approach addresses the urgent need for renewable energy sources by leveraging the enzymatic hydrolysis of canola oil using *Candida rugosa* lipase under both batch and continuous flow conditions. This step effectively transforms triglycerides into free fatty acids with remarkable conversion and selectivity rates exceeding 99%. The process then advances to a continuous-flow heterogeneous catalytic hydrogenation employing a Pd/C catalyst, producing saturated fatty acids, or alternatively, a continuous ozonolysis reaction leading to mono- and dicarboxylic acids. The final stage involves enzymatic photodecarboxylation using *Chlorella variabilis* fatty acid photodecarboxylase (CvFAP), resulting in the generation of long- and medium/short-chain alkanes suitable for low-oxygen-content fuel production. The approach not only offers a greener alternative to traditional methods but also aligns with the principles of green chemistry by reducing operational time, waste generation, and energy consumption. This work sets a precedent for the valorization of vegetable oils into high-value fuels, providing a viable pathway for industrial-scale renewable energy production and contributing to global sustainability goals.

Received 19th December 2024
Accepted 17th May 2025

DOI: 10.1039/d4su00813h

rsc.li/rscsus



Sustainability spotlight

Current fossil-based fuel production systems contribute to resource depletion and climate change, underscoring the urgent need for sustainable alternatives. This work addresses the potential of a chemo-enzymatic cascade for the valorization of renewable feedstocks. By integrating enzyme-driven and continuous-flow catalytic processes, the approach enhances process efficiency. These improvements align with the United Nations Sustainable Development Goals (SDGs), particularly SDG 7 (Affordable and Clean Energy), SDG 12 (Responsible Consumption and Production), and SDG 13 (Climate Action), ensuring that renewable resources are effectively harnessed to contribute to a cleaner, more sustainable energy future.

1. Introduction

The stark contrast between the burgeoning energy sector and the rapid depletion of nonrenewable fossil fuels is a cause for concern. Projections suggest that by 2042, black coal may stand as the sole remaining fuel source, underscoring the urgent need for a transition to greener energy alternatives.¹⁻³

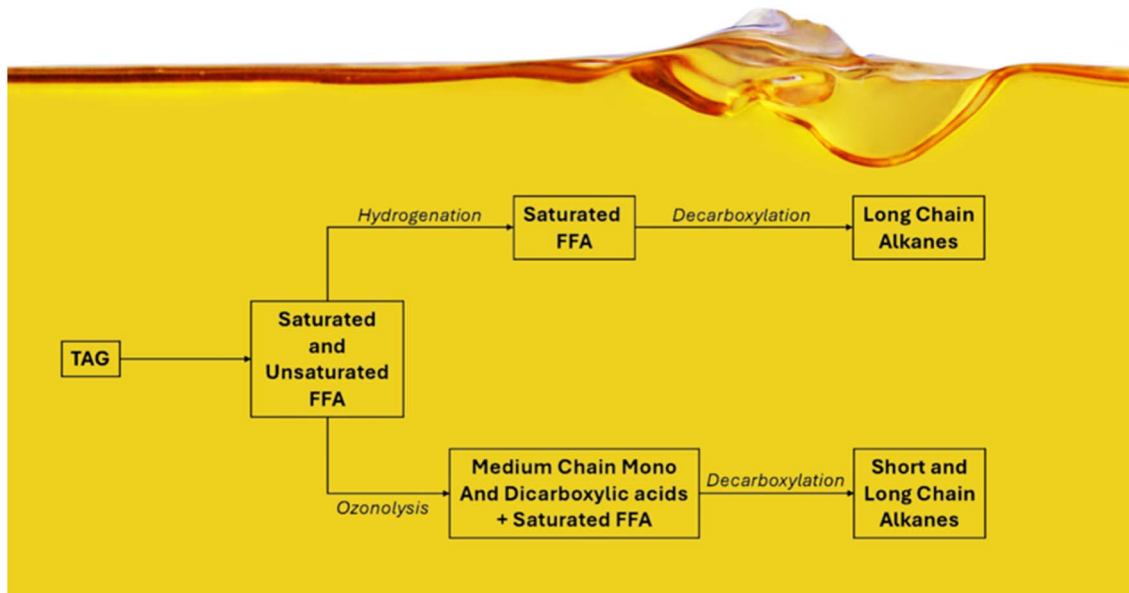
Biomass-derived hydrocarbon fuel has emerged as a promising sustainable substitute for traditional fossil fuels, particularly as it constitutes over 60% of commercial aviation fuel.⁴ This biofuel boasts renewability, low toxicity, and biodegradability, rendering it an environmentally sound choice. Additionally, its combustion characteristics closely mimic those of fossil fuels, granting it superiority over methyl/ethyl ester-based biodiesel in terms of stability and non-corrosiveness. Such attributes make it ideal for surrogate fuel models, further solidifying its position as a viable solution to our energy needs.^{5,6}

The hydrolysis of vegetable oils, including canola, palm, and soybean oil—rich in long-chain triglycerides—is a well-established method for producing biofuels like biodiesel.⁷⁻¹³ Moreover, the hydrolysis of vegetable oils can yield low-oxygen fuels, such as hydrocarbon-based ones, through subsequent

^aBiocatalysis and Organic Synthesis Group, Instituto de Química, Universidade Federal do Rio de Janeiro, Rio de Janeiro, 21941909, Brazil. E-mail: rodrigosouza@iq.ufrj.br

^bLaboratório de Microbiologia Molecular e Proteínas, Instituto de Química, Universidade Federal do Rio de Janeiro, Rio de Janeiro, 21941909, Brazil

† Electronic supplementary information (ESI) available. See DOI: <https://doi.org/10.1039/d4su00813h>



Scheme 1 Chemical pathways towards short and long chain alkanes.

hydrogenation and decarboxylation processes. Medium/short chain hydrocarbons can also be obtained if the ozonolysis reaction of the free fatty acids is used in place of hydrogenation (Scheme 1).

Conventional hydrolysis processes typically necessitate harsh operational conditions involving high pressures, temperatures, or acidic/alkaline environments, resulting in yields of the desired product exceeding 99%. However, biocatalytic systems present a greener alternative, offering comparable efficiency while mitigating some drawbacks associated with chemical methods.^{14,15}

Among the enzymes utilized in vegetable oil hydrolysis, enzymes like lipase (EC 3.1.1.3) exhibit several advantages. They accelerate the reaction, enabling it to proceed under milder conditions, yield more specific products with equivalent efficiency, and do not rely on cofactors.¹⁶ Nevertheless, the cost of enzymes can sometimes hinder the scalability of the process.

Another category of enzymes closely linked to hydrocarbon fuel synthesis is photodecarboxylases. This recently identified group of photoenzymes possesses the remarkable ability to convert fatty acids (C_n) into their corresponding hydrocarbons (C_{n-1}) under continuous light exposure. Numerous studies focus on this enzyme group, particularly *Chlorella variabilis* fatty acid photodecarboxylase (CvFAP), underscoring its immense potential for biotechnological applications within the biofuel sector.^{17,18}

So far, there hasn't been a biocatalytic alternative for the hydrogenation or ozonolysis reactions of fatty acids, but greener methodologies can be achieved through the utilization of continuous-flow reactors, where hydrogen (H₂) is generated *in situ* via water electrolysis or small amounts of O₃ are needed for the cleavage of double bonds.¹⁹⁻²⁴ Also, continuous-flow systems offer a notable advantage in compartmentalization, allowing for seamless integration of chemical and biocatalytic reactions within a single reaction stream. This capability facilitates the

development of cascade reactions, thereby enhancing the versatility and efficiency of the synthesis process.

Chemo-enzymatic cascade reactions present an intriguing strategy for converting renewable resources into high-value products. Recent research has highlighted the effectiveness of chemo-enzymatic cascades in transforming vegetable oils into fine chemical products.^{25,26} This approach enables the amalgamation of various catalysts, both chemical and enzymatic, combining multiple individual steps into a sequential process. This consolidation enhances the overall efficiency of chemical and enzymatic processes by reducing the number of required work-up operations, minimizing time consumption, and streamlining labor efforts.

In line with this approach, this study aims to utilize Canola oil (*Brassica napus* L.) in a chemo-enzymatic cascade to produce hydrocarbon fuel. The process begins with the enzymatic hydrolysis of Canola oil using *Candida rugosa* lipase under both batch and continuous flow conditions. The choice of working with the free enzyme instead of an immobilized one was based only on the economic aspect of the process. While immobilized enzymes offer advantages in terms of reusability, their production and application can be cost-prohibitive in developing countries. This is followed by a continuous-flow heterogeneous catalytic hydrogenation employing a Pd/C catalyst to produce saturated fatty acids or a continuous ozonolysis reaction leading to mono and dicarboxylic acids. Finally, these saturated carboxylic acids are subjected to enzymatic photodecarboxylation to yield long-and medium/short chain alkanes, serving as raw materials to produce low-oxygen-content fuels.

2. Materials and methods

2.1. Chemical materials

Canola oil from Purilev, tris base (Sigma-Aldrich), HCl 37% (Vetec Química), Kanamycin (Fluka), Bradford protein assay



reagent (Bio-Rad), methyl sulfoxide (Tedia), ethyl acetate (Tedia), ethanol 99.5% (Vetec Química), methanol (Vetec Química), sodium sulphate anhydrous (Vetec Química), palmitic acid (Sigma-Aldrich), and a PierceTM BCA Protein Assay Kit (ThermoFisher Scientific) were used. Thin layer chromatography (TLC) analyses were performed on aluminum sheets pre-coated with silica gel 60 F254 from Merck (Darmstadt, Germany).

2.2. Equipment

An analytical balance mettler toledo, magnetic stirrer heating plate – Model 753A – FISATOM, Asia System 110 Continuous Flow – Syrris, Orbital Shaker Incubator Marconi, Shimadzu GC-2010 MS, Shimadzu GC-2010 FID, PTFE-coil (1/16), Portable digital KR812 luximeter (until 200 000 lux), Ultrasonic Sonicator VIBRA-CELL VCX 500 Sonics (USA), Branson 1510R-MT Ultrasonic Cleaner, H-Cube[®] Mini Plus and Pd/C 10% CatCart (ThalesNano) were used. NMR spectra were recorded on a Bruker 400 MHz spectrometer in a deuterated solvent. The values of chemical shifts (δ) are expressed in ppm with reference to tetramethylsilane (TMS) for ^1H NMR and the chloroform signal for ^{13}C NMR. Coupling constants (J) are expressed in Hertz (Hz).

2.3. Enzymes

Commercially available *Candida rugosa* lipase (4010 U g⁻¹), also called *Candida cylindraea* (CCL), was purchased from Fluka analytical. The CvFAP gene was housed in *Escherichia coli* DH5 α strains, and the enzyme was produced in transformed competent *E. coli* BL21 (DE3) cells with this plasmid, as described in previous work.¹⁷ Kanamycin, obtained from Fluka, was the antibiotic used in the process.

2.4. Analysis

Gas chromatography analyses were conducted on a Shimadzu GC-2014 MS or GC-2010 FID both with a DB-5HT column (30 m \times 0.25 mm \times 0.25 μm) (Agilent Technologies).

2.4.1. Gas chromatography-mass spectrometry analysis. GC-2014 MS method: Injection temperature 280 °C, injection split ratio 1 : 50, helium (99.9992% purity) as the carrier gas at 2 mL min⁻¹ in constant flow mode, pressure 92.0 kPa, column flow 1.09 mL min⁻¹. The oven temperature setting was 130 °C for 1 min, heating at 10 °C min⁻¹ to 200 °C for 1 min, and then heating at 15 °C min⁻¹ to 300 °C, solvent cut time 3 min. Mass spectra were obtained in scan mode (45–800 Da).

2.4.2. Gas Chromatography-FID analysis. CG-2010 FID method: Injection temperature 350 °C, injection split ratio 1 : 10, hydrogen as the carrier gas with a pressure of 112.9 kPa and column flow rate of 2.60 mL min⁻¹. The oven temperature setting was 100 °C for 1 minute, then heated at 20 °C min⁻¹ to 150 °C, then heated at 10 °C min⁻¹ until 180 °C for 6 min, and then heated at 25 °C min⁻¹ to 370 °C for 10 min. Flame temperature 380 °C. Conversions were calculated by using the ratio of the sum of product areas to total analyte areas (products and starting material), and selectivity towards FFA was calculated by using the ratio of fatty acid area to the sum of areas of

products generated in the reaction: diacyl glycerol, monoacyl glycerol and fatty acid.

2.5. Preparation of the biocatalysts

The enzyme expression methodology followed the protocol outlined by Huijbers and colleagues (2018).²⁷ Following CvFAP expression, the whole-cell biocatalyst (CvFAP_WC) was prepared as described in previous work.¹⁸

2.6. Canola oil hydrolysis

2.6.1. Enzyme concentration by activity assay. The hydrolysis activity of CRL was measured by using a hydrolysis reaction adapted from Freire *et al.*²⁸ The reaction mixture consists of olive oil (5% m/v) emulsified with Arabic gum (5% m/v) in 100 mM sodium phosphate buffer (pH 7.0). Twenty milliliters of the emulsion were mixed with 10 mg of free enzyme. After incubation for 30 minutes at 37 °C and 180 rpm on a shaker, the reaction was stopped by adding 20 mL of ethanol/acetone solution (1 : 1 v/v). Titration with 0.029 mol L⁻¹ sodium hydroxide was performed using an automatic titrator until reaching pH 11.0. Blank samples were prepared without enzyme addition, and after incubation, 20 mL of ethanol/acetone solution was added. All analyses were performed in triplicate, and the arithmetic means of the values obtained were used to calculate enzymatic activity (Table S1 in the ES[†]).

2.6.2. Parameter improvement under batch conditions. Hydrolysis reactions were performed in a total 2 mL reaction volume composed of water and canola oil; these components were added to a transparent vial glass (4 mL). The lipase load and the oil-water ratio were evaluated, and the reaction was carried out at 200 rpm and 40 °C for 2 h, on a stirring and heating plate. To analyze the samples of hydrolysis reactions by GC, they were prepared by sampling 20 μL of the oil layer, and then it was extracted using 400 μL of heptane and 100 μL of brine. For higher resolution in chromatograms, 200 μL of the organic layer was silanized using 100 μL BSTFA (*N,O*-bis(trimethylsilyl)trifluoroacetamide) and 100 μL of chloroform. The media were heated on a stirring plate at 60 °C for 30 min, and then diluted with 350 μL of heptane and 350 μL of chloroform.

2.6.3. Parameter improvement under continuous flow conditions. Four different setups were studied to improve the water-oil mixture to reach the best hydrolysis yields. In all setups, oil and water, containing lipase, were pumped separately into one of the following reactors: in setup A, a steel column reactor, whose length and diameter are 116.06 and 10.86 mm respectively, filled with 3.0 mm steel spheres, which were used as static mixers; in setup B, a PTFE coil, whose volume is 12 mL and its external and internal diameters are 1/8' and 1/16' respectively, intended to create a proper reaction medium by using finely segmented water-oil frames. Additionally, in systems C and D, an ultrasound bath, Branson, operating at 40 kHz was employed to enhance mixing inside the reactors used in setups A and B. This is done by using ultrasonic waves, which generate cavitation, promoting efficient dispersion of reactants, improving mass transfer, and accelerating



reaction kinetics. In order to accomplish the reaction in these setups in appropriate residence times, setups A and C used a total flow of $400 \mu\text{L min}^{-1}$, while setups B and D used a total flow of $163.3 \mu\text{L min}^{-1}$, and oil–water ratios and enzyme concentration were changed for evaluation. ESI Fig. S1† shows setup D, representing the experimental setups. The same procedure to prepare samples for CG analysis in the last section was used.

2.7. Hydrogenation of the FFA mixture derived from canola oil

2.7.1. Batch. For the hydrogenation experiments, the FFA mixture was extracted with hexane and brine, and then the organic layer was evaporated under low pressure. After the workup, the hydrogenation of canola oil-derived fatty acids in batch mode was carried out using a Pressure Reactor miniclave drive – Buchiglas (Büchi AG – Switzerland) (see Fig. S2 in the ESI†). The solution (100 mL) of canola oil-derived fatty acids in ethanol 99.5% (1 mg mL^{-1}) was added to a 500 mL glass reactor with 5 mg of the 10% Pd/C catalyst. The pressure of hydrogen was 10 bar. The reaction mixture was stirred (200 rpm) at 25°C for 60 min. Then, the shaking was stopped, and the hydrogen pressure was released. The mixture was filtered to remove the catalyst and was analyzed by gas chromatography (see Table S2 in the ESI†).

2.7.2. Continuous flow. Continuous-flow experiments were performed in a high-pressure continuous-flow hydrogenator reactor H-Cube® Mini Plus (ThalesNano; see Fig. S3 in the ESI†). The solution of canola oil-derived fatty acids in ethanol 99.5% (1 mg mL^{-1}) was pumped through a reactor module in which a 70 mm catalyst cartridge packed with 250 mg of 10% Pd/C catalyst was installed. The total flows were 0.5 and 2.3 mL min^{-1} equivalent to a residence time of 100 and 20 s, respectively, with the temperature controlled at 30 and 50°C . Then, the samples were analyzed by gas chromatography.

2.8. Ozonolysis

2.8.1. Batch ozonolysis of commercial oleic acid. Oleic acid (111 mg) and acetone–water, 95 : 5 v/v (7.55 mL) were added to a 50 mL jacketed reaction vessel (Fig. S6 in the ESI†). The solution was cooled to 0°C and treated with ozone for 15 min. Then, oxygen was bubbled at a flow rate of 500 mL min^{-1} for 20 min. Subsequently, for ozone destruction, quenching was performed with potassium iodide solution (5% m/v). The product was dried under vacuum, and 5 mg was derivatized with $100 \mu\text{L}$ of BSTFA for 30 min at 60°C . At the end, the solution was diluted to 1 mL with CHCl_3 for GC-FID analysis.

2.8.2. Batch hydrolysis and ozonolysis of canola oil. CRL (0.01% m/v), 1 mL of canola oil, and 4 mL of water were added to a 50 mL jacketed reaction vessel. The reaction was processed for 4 h at 40°C . Then, 57 mL of acetone was added. The temperature was lowered to 0°C and the solution was treated with ozone until total ozonide formation (confirmed by TLC), at around 40 min. Subsequently, it was followed by O_2 purge for complete oxidation at 500 mL min^{-1} for 80 min. Subsequently, the product was dried under vacuum, and 5 mg was derivatized

with 100 μL of BSTFA for 30 min at 60°C . At the end, the solution was diluted to 1 mL with CHCl_3 for GC-FID analysis.

2.8.3. Hybrid batch-flow ozonolysis. Oleic acid (111 μL) or an FFA mixture derived from canola oil (without any workup) and acetone to ensure a 95 : 5 v/v proportion of acetone–water was pumped to a CSTR reactor at 0°C , where it was treated with ozone for 20 min. Next, it meets, through a T mixer, with acetone–water 95 : 5 v/v solution that was pumped into a tube-in-tube reactor permeated by oxygen at 6 bar followed by a 12 mL coil at 0°C through a thermocirculator (Scheme S2 and Fig. S7 in the ESI†). The system pressure was 4 bar. The product was then dried under vacuum. Then 5 mg was derivatized with 100 μL BSTFA for 30 min at 60°C , and the solution was then diluted to 1 mL with CHCl_3 for GC-FID analysis. For product purification, hexane was added to the reaction mixture, and azelaic acid was extracted using hot water. The aqueous phase was then reduced under mild heating conditions, leading to the crystallization of azelaic acid (AA) as white crystals (Fig. S8 in the ESI†). These crystals were subsequently filtered, washed multiple times with cold water, and dried to obtain the purified product.

Simultaneously, the hexane layer containing pelargonic acid was dried over anhydrous sodium sulfate (Na_2SO_4), filtered, and concentrated to yield a viscous oily liquid (Fig. S9 in the ESI†). The isolated yields for pelargonic acid and azelaic acid were determined to be 88.9% and 48.8%, respectively.

2.9. Enzymatic photodecarboxylation of stearic and pelargonic acids in batch

2.9.1. Expression of CvFAP and preparation of the whole-cell biocatalyst. The plasmid construction consists of a $6 \times$ His-tag, thioredoxin (TrxA) tag, tobacco etch virus (TEV) protease cleavage site, and the gene coding for residues 62–654 of CvFAP (GenBank: KY511411.1) cloned into a pET28a expression vector and transformed into *Escherichia coli* BL21 (DE3) competent cells sequentially.²⁹ For expression, a single colony was inoculated into 10 mL of LB medium with kanamycin ($50 \mu\text{g mL}^{-1}$) and grown overnight at 37°C and 200 rpm. The pre-culture was then used to inoculate a 2 L Erlenmeyer flask containing 500 mL of fresh TB-kanamycin medium (1 : 100 dilution), and the culture was incubated at 37°C and 200 rpm until reaching an OD_{600} of ~ 0.6 –0.8. Protein expression was then induced by the addition of IPTG (0.5 mmol L^{-1}), and the culture was incubated at 17°C and 200 rpm for 21 hours. Following induction, the cells were protected from direct light exposure. Cells were harvested by centrifugation at 11 000 rpm for 15 minutes at 4°C , and the pellet was washed once with Tris–HCl buffer (50 mm, pH 8, containing 100 mm NaCl). The resulting whole-cell catalyst (CvFAP_WC) was resuspended in the same buffer containing 20% glycerol for cryopreservation in an ultrafreezer (-80°C) for further assays. Cells were resuspended at the desired pH, depending on the fatty acid substrate used in the photodecarboxylation step.

2.9.2. Photodecarboxylation reaction conditions. Photodecarboxylation reactions were carried out using the freshly prepared CvFAP_WC suspension. For stearic acid, the whole-cell suspension was adjusted to pH 8.5 in 0.1 mol L^{-1} phosphate



buffer, whereas for pelargonic acid, a pH of 6.0 was used, as described by Samire *et al.*³⁰ (2023) to enable medium-chain acid conversion. The substrate was added to the reaction as a 30% organic phase (typically in DMSO), mixed with 70% aqueous phase (CvFAP_WC suspension for a final concentration of 11 mg mL⁻¹). The final reaction volume was typically 1 mL in sealed borosilicate vials. Reactions were irradiated for 5–30 minutes in a ThalesNano PhotocubeTM equipped with four 16 W 365 nm UV panels, ensuring full exposure from all sides. The temperature was maintained at 37 °C using a LAUDA thermocirculator, and stirring was applied when necessary to ensure homogeneity.

After irradiation, the samples were extracted with ethyl acetate, dried over anhydrous sodium sulfate, and analyzed by GC-FID or GC-MS. Conversions were calculated by integration of the substrate and product peaks. All reactions were conducted in triplicate.

3. Results and discussion

Initially, the hydrolysis reactions in batch mode were screened using the lipase from *Candida rugosa* (CRL), also called *Candida cylindracea* (CCL) since this is a cheap and efficient enzyme for processing vegetable oils. In a recent study, Yang and colleagues showcased the application of CRL to produce n-3 polyunsaturated fatty acids, achieving interesting results for this enzyme.¹⁰ Reaction conditions were evaluated by analysis of reactional parameters, such as the enzyme loading and oil–water ratio, for 2 h (Table 1). All reactions were performed in triplicate. The hydrolytic efficiency of CRL was determined by GC-FID through the area percentage correlation between the triacylglycerol (TAG) (starting material), diacylglycerol (DAG)

and monoacylglycerol (MAG) intermediates, and the free fatty acid (FFA) products.

Excellent conversions and selectivity towards FFA (>99%) were observed on reducing the amount of CRL enzyme up to 0.1% (entries 1 to 4, Table 1). Further reduction to 0.05% leads to a slight decrease in conversion to 92% (entry 5, Table 1), with selectivity still above 95%. Maintaining the same CRL enzyme amount (0.1% w/v) while increasing the oil concentration in the mixture (1 : 1 v/v), resulted in a good conversion and selectivity of 93%, thus significantly boosting process productivity by working on higher concentration media. Shorter reaction times were evaluated but do not lead to better results when compared to those presented in Table 1.

After this initial reaction assessment, we decided to explore the benefits of continuous-flow chemistry for the hydrolysis of canola oil mediated by the free CRL enzyme. The idea was to take advantage of the increased mass transfer to enhance the oil–water emulsion, thereby increasing process productivity by converting a larger quantity of TAG in a shorter reaction time. We have studied two different reactor types (tubular reactor and packed bed filled with 3 mm metallic spheres) with and without ultrasound irradiation. The results are presented in Table 2 (reactor A = tubular reactor without an ultrasound bath/reactor B = packed bed reactor filled with 3 mm metallic spheres without an ultrasound bath/reactor C = tubular reactor with an ultrasound bath/reactor D = packed bed reactor filled with 3 mm metallic spheres with an ultrasound bath).

Data in Table 2 present comparative analysis of enzymatic reaction performance across different reactors, oil-to-water ratios, and enzyme loadings, emphasizing selectivity and free fatty acid (FFA) conversion efficiency. Reactor types A, B, C, and D show varying performances, with Reactor D consistently

Table 1 Reaction optimization for canola oil hydrolysis catalyzed by the CRL enzyme^a

Entry	Enzyme loading (%)	Hydrolytic activity (U g ⁻¹)	Oil–water ratio	Selectivity FFA ^b (%)	
				Conv. ^b (%)	
1	2	69.4	1 : 4	>99	>99
2	0.5	15.8	1 : 4	>99	>99
3	0.2	6.3	1 : 4	>99	>99
4	0.1	3.2	1 : 4	>99	>99
5	0.05	1.6	1 : 4	92 ± 2	95 ± 1
6	0.1	3.2	1 : 3	97 ± 1	97 ± 1
7	0.1	3.2	1 : 2	94 ± 2	94 ± 2
8	0.1	3.2	1 : 1	93 ± 1	93 ± 2

^a Reaction conditions: the reaction was carried out in a transparent flask reactor containing a reaction mixture of water and canola oil (2 mL total volume). The mixture was stirred at 200 rpm and maintained at 40 °C for 2 hours. ^b Conversion and selectivity were determined by gas chromatography (GC) through the integration of chromatographic peak areas. Conversions were calculated by using the ratio of sum of product areas to total analyte areas (products and starting material), and selectivity FFA (%) is defined as the relative GC-FID area of free fatty acids among all acylglycerol species (TAG, DAG, MAG, and FFA).



Table 2 Hydrolysis of canola oil under continuous-flow conditions catalyzed by the CRL enzyme in different reaction setups^a

Entry	Reactor	Oil–water ratio	Enzyme loading (%)	Selectivity FFA ^b (%)	Conv. ^b (%)
1	A	1 : 1	0.1	63.5 ± 0.2	40.8 ± 0.1
2	B			58 ± 2	30 ± 1
3	C			62 ± 1	47 ± 2
4	D			75 ± 1	67 ± 2
5	A	1 : 2	0.1	55 ± 2	31 ± 2
6	B			56 ± 2	22 ± 2
7	C			66 ± 3	49 ± 2
8	D			77 ± 1	63 ± 3
9	A	1 : 3	0.1	61 ± 1	38 ± 1
10	B			70 ± 2	43 ± 1
11	C			75 ± 2	65 ± 1
12	D			85 ± 1	79 ± 1
13	A	1 : 4	0.1	66 ± 1	54 ± 1
14	B			86 ± 1	70 ± 1
15	C			75 ± 1	68 ± 1
16	D			89 ± 1	86 ± 2
17	A	1 : 4	0.5	71 ± 1	52 ± 1
18	B			76 ± 2	46 ± 3
19	C			97 ± 1	95 ± 1
20	D			93 ± 1	94 ± 1

^a Reaction conditions: a container with CRL (3.17 U·g⁻¹ of initial hydrolytic activity, for entries 1–16 and 15.85 U g⁻¹ for entries 17 to 20) in water, while pump B contained canola oil. The starting material solutions were introduced into the reactor system (A, B, C, or D) via a T-mixer. Reactions were performed at 40 °C with a residence time of 30 minutes. ^b Conversion and selectivity were determined by gas chromatography (GC) through the integration of chromatographic peak areas. Conversions were calculated by using the ratio of sum of product areas to total analyte areas (products and starting material), and selectivity was calculated by using the ratio of fatty acid area to the sum of areas of products generated in the reaction.

achieving the highest selectivity and conversion under all tested conditions. For instance, at an oil-to-water ratio of 1 : 4 and an enzyme loading of 0.1%, Reactor D outperforms others with selectivity and conversion rates of 89 ± 1% and 86 ± 2%, respectively (Table 2, entry 16).

As the oil-to-water ratio increases from 1 : 1 to 1 : 4, both selectivity and conversion improve across all reactors, suggesting that higher water content creates a reaction environment conducive to enhanced enzyme activity or better substrate interaction. Additionally, increasing the enzyme loading from 0.1 to 0.5% further boosts performance, particularly for the more efficient reactors like C and D (Table 2, entries 15, 16, 19 and 20). At the highest enzyme loading and oil-to-water ratio tested, Reactor C achieves 97 ± 1% selectivity and 95 ± 1% conversion (Table 2, entry 19), closely followed by Reactor D with 93 ± 1% selectivity and 94 ± 1% conversion (Table 2, entry 20).

The superior performance of reactors C and D, equipped with ultrasound baths, highlights the significant benefits of ultrasound in enhancing mass transfer during reactions involving water–oil mixtures. Ultrasound generates acoustic cavitation, creating microbubbles that collapse and produce localized high-energy conditions. These effects disrupt interfacial barriers between immiscible phases, improving emulsification and ensuring more efficient mixing of water and oil. Additionally, the mechanical vibrations induced by ultrasound enhance the diffusion of reactants to the enzyme's active site, promoting faster reaction rates.¹² This technique is particularly advantageous in enzymatic processes, as it can improve substrate availability without compromising enzyme stability

under carefully controlled conditions. The consistent out-performance of reactors C and D suggests that ultrasound integration into reactor design can significantly optimize biphasic reaction systems, making it a valuable tool for continuous-flow biocatalysis.

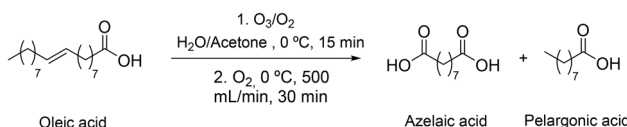
The study underscores the critical role of process optimization in enzymatic systems. Increasing the oil-to-water ratio and enzyme loading consistently enhances reaction performance, likely due to improved hydration of the enzyme and better substrate availability. Reactor D emerges as a promising candidate for continuous-flow applications due to its robust performance, although the scalability of its design, enzyme stability, and associated costs require further evaluation.

The continuous systems provide several advantages in process safety, such as superior control over high pressure and temperature and effectively addressing the limitations associated with mass/heat transfer due to their high surface area to volume ratio and shorter diffusion path length. Additionally, continuous reactors reduce reaction times, and their low processing volume improves waste minimization, reflecting the principles of green chemistry, thereby greatly enhancing efficiency and productivity.³¹

After establishing the hydrolysis protocol, the next step was to work on the modification of the fatty acid chain by either cleavage of the double bond by ozonolysis or reduction by a hydrogenation reaction.

To begin our investigation, we explored the results of the ozonolysis reaction under batch conditions. Initially, we adapted a batch ozonolysis setup based on a protocol described in the literature, modifying it to align with our experimental





Scheme 2 Batch ozonolysis of commercial oleic acid.

requirements. To simplify the system and reduce complexity, we opted for a non-pressurized setup using air instead of oxygen as the feed gas for ozone generation. This approach was facilitated by an ozone generator with a capacity of 10 g of ozone per hour at a flow rate of 1.3 mL min^{-1} .

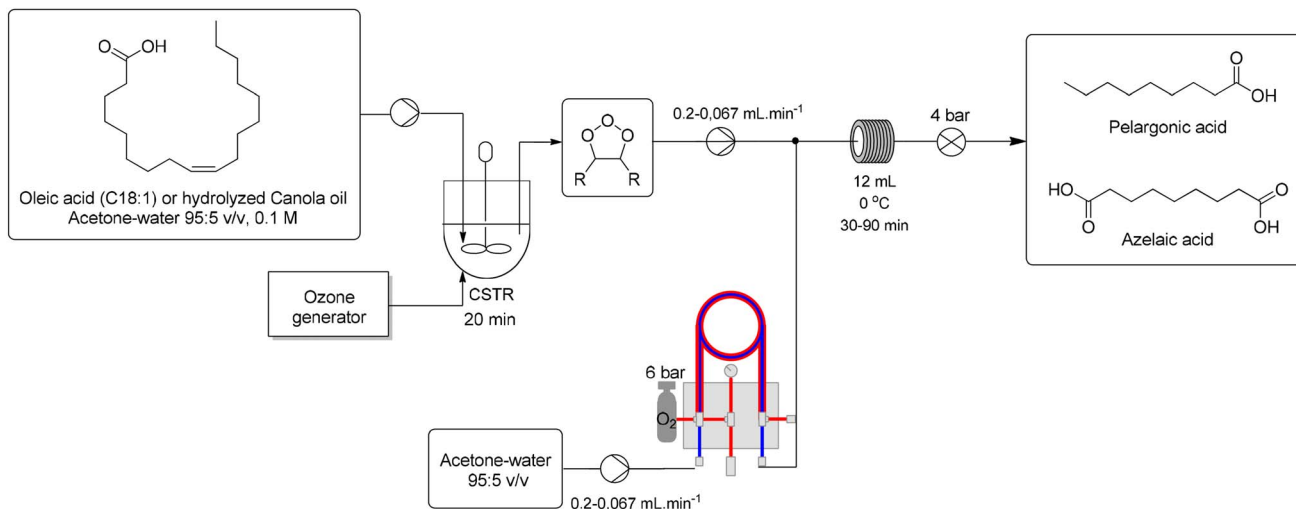
The ozonolysis reaction was initially conducted using commercial oleic acid (0.1 mol L^{-1} in acetone-water, 95 : 5 v/v) as the substrate. The reaction was carried out until formation of ozonide and oleic acid consumption, as confirmed by thin-layer chromatography (TLC) (see Fig. S12 in the ESI†) and subsequent CG-FID, which occurred within 15 min of ozone treatment. Subsequently, the reaction mixture was subjected to oxygen treatment at a flow rate of 500 mL min^{-1} for 30 min. This process yielded azelaic and pelargonic acids with conversion and selectivity exceeding 99% (Scheme 2) (see Fig. S6† for the batch ozonolysis setup and Fig. S14† for the chromatographic profile). These results demonstrate the efficiency of the adapted

batch ozonolysis setup, even under non-pressurized conditions with air as the feed gas.

The same experimental setup used for the ozonolysis reaction with commercial oleic acid was adapted to process the product obtained from canola oil hydrolysis. Following the continuous-flow hydrolysis of canola oil under the conditions outlined in Table 2 (entry 19), the resulting product was collected, and acetone was added to the reaction mixture to achieve the appropriate solvent ratio for the subsequent ozonolysis reaction. The reaction temperature was lowered to $0^\circ C$, and the solution was treated with ozone until the formation of the ozonide was confirmed by thin-layer chromatography (TLC), requiring 40 min due to the increased complexity of the starting material. This step was followed by an oxygen purge (500 mL min^{-1} for 80 min), which resulted in complete oxidation to the desired carboxylic acids with $>99\%$ conversion and 92% selectivity (see the ESI for the chromatographic profile – Fig. S15†). This methodology is unprecedented, enabling the production of mid-chain carboxylic acids, including azelaic, pelargonic, hexanoic, and malonic acids, without requiring intermediate workup steps. Approximately 1 gram of products was obtained in just two hours under mild conditions, facilitated by enzymatic catalysis.

Due to the limitations of our ozone generator, which cannot operate under pressure, it was not feasible to adapt the batch

Table 3 Combined batch and continuous-flow ozonolysis of the commercial oleic acid and FFA mixture derived from canola oil



Entry	Starting material	Oxidation R. t. (min)	Conv. ^c (%)	Selectivity ^c (%)
1 ^a	Oleic acid	30	>99	84
2 ^a	Oleic acid	40	>99	93
3 ^b	FFA mixture	40	>99	75
4 ^a	Oleic acid	50	>99	92
5 ^b	FFA mixture	50	>99	82
6 ^b	FFA mixture	60	>99	89

^a Reaction conditions: oleic acid as starting material. ^b Reaction conditions: reaction media originated by the enzymatic hydrolysis reaction.

^c Conversions were calculated by using the ratio of the sum of product areas to total analyte areas (products and starting material), and selectivity was calculated by using the ratio of medium and short chain fatty acid area to the sum of areas of products generated in the reaction; R. t. (residence time) (see ESI Fig. S16–S21).



ozonolysis conditions to a continuous-flow system. Instead, we developed a hybrid approach: the initial ozonide formation was conducted under batch conditions, while the oxidation step was carried out in a continuous-flow system using a tube-in-tube (TiT) reactor to address safety concerns (see the ESI, Figure S7† for the flow ozonolysis setup). This combined strategy allowed us to complete the ozonolysis of oleic acid with good yields and in shorter reaction times. The results of this hybrid protocol are presented in Table 3.

Batch ozonide formation was set to 20 min to ensure complete consumption of the free fatty acid mixture. After this time, reaction media were pumped through a T-mixer against a reaction stream which has passed through a TiT reactor to saturate the solvent mixture (acetone/water) with O₂. The combined streams go into a tubular reactor at 0 °C where the oxidation reaction takes place. Different residence times were used for the oxidation step and a full conversion of the FFA was always observed. Shorter residence times led to a decrease in the carboxylic acid content, but from 30 to 60 min similar selectivity towards pelargonic and azelaic acids was observed, and at 40 min, the best results were observed for oleic acid (entry 2, Table 3). When working with the products coming from enzymatic hydrolysis, a more complex mixture of starting materials is used, since linolenic and linoleic acid are also present in canola oil. In this case a longer residence time is needed to accomplish a good selectivity (entry 6, Table 3). The isolated yield for this reaction is 70% due to difficulties in the isolation of azelaic acid which can still be observed in the aqueous phase. In this way, we were able to develop an interesting two step hydrolysis/

ozonolysis protocol for valorization of FFA, with an overall conversion of 94% after 80 min for oleic acid and 110 min for canola oil (see Fig. S21 in the ESI†).

As mentioned, we were also interested in the modification of the unsaturated or polyunsaturated FFA by the hydrogenation reaction, affording long chain saturated free fatty acids as major products. At this point we have decided to move directly to the continuous-flow protocol using the product obtained from the enzymatic hydrolysis as the starting material for our evaluation. The optimization of the hydrogenation reaction was done using an H-Cube Mini reactor. The canola oil-derived fatty acid solutions were pumped into the system at different flow rates, resulting in 20 and 100 s residence times (r.t.). Reaction temperatures of 30 and 50 °C were tested. The system pressure varied according to the chosen temperature and flow rate, ranging between 15 and 30 bar. Two reaction parameters that influence the conversion of continuous flow hydrogenation of canola oil-derived fatty acids were evaluated with the performance of a central composite rotational design (CCRD) with four axial points and two repetitions of the centroid point (see Table S3 and Fig. S4, S5 in the ESI†). The independent variables were temperature (25.9, 30, 40, 50 and 54.1 °C) and residence time (39.6, 50, 75, 100 and 110.4 s), and the response variable was conversion (%). The results obtained are presented in Table 4.

Based on the results obtained the increase in residence time led to higher conversion towards the desired product. But, along with residence time, the increase in reaction temperature from ambient to 40 or 50 °C also has an impact on the conversion observed. The best results were obtained at residence times higher than 75 s and temperatures between 40 and 50 °C (entries 4, 8–10, Table 4). The statistical analysis of data (see Fig. S4 and S5 in the ESI†) demonstrated that the empirical model ($R^2 = 0.95$) could be predictive. The factors considered significant (p -value < 0.05) by the analysis of variance (ANOVA – Table S3 in the ESI†) involved both temperature and residence time variables, with positive effects in the conversion of the hydrogenation reaction. This finding aligns with the existing literature²⁷ highlighting the benefits of flow hydrogenation techniques compared to conventional batch methods, such as real-time analysis and the ability to create quicker, multi-step, and cascade synthetic procedures.

With the long and short chain carboxylic and dicarboxylic acids in hand we moved towards our final step, enzymatic photodecarboxylation. Previously, our research group has found excellent conditions for long chain fatty acid photodecarboxylation using very short reaction times under irradiation of violet light.¹⁸ In this way, the present approach aimed to propose the photodecarboxylation of a hydrogenated FFA mixture derived from canola oil, a product obtained in the

Table 4 Hydrogenation of the canola oil-derived fatty acids under continuous-flow conditions^a

Entry	T (°C)	R. t. ^b (s)	Conversion ^c (%)
1	30.0	50.0	75
2	30.0	100.0	88
3	50.0	50.0	79
4	50.0	100.0	95
5	25.9	75.0	70
6	54.1	75.0	87
7	40.0	39.6	75
8	40.0	110.4	95
9	40.0	75.0	92
10	40.0	75.0	92

^a Reaction conditions: solution (100 mL) of canola oil-derived fatty acids in ethanol 99.5% (1 mg mL⁻¹), 250 mg of Pd/C 10% catalyst cartridge (Thales Nano), 15–30 bar H₂. ^b Residence time. ^c Conversion was determined by gas chromatography (GC) through the integration of chromatographic peak areas. Conversion was calculated as the ratio of the sum of product areas to total analyte areas (product and starting material).

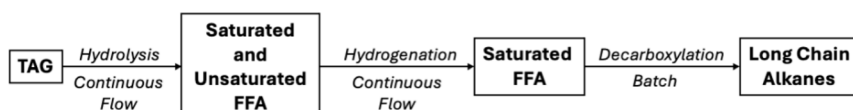


Fig. 1 Sequential hydrolysis–hydrogenation–decarboxylation.



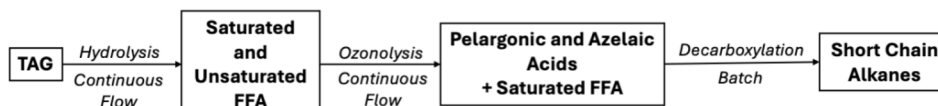


Fig. 2 Sequential hydrolysis–ozonolysis–decarboxylation.

present reactional cascade. A complete photodecarboxylation conversion (>99%) was obtained utilizing a 50 W violet LED lamp (397 nm) with a reaction time of 5 min (see Fig. S25–27 in the ESI†) indicating its high efficiency for alkane production. Although the capacity of *CvFAP* to convert fatty acids into alkanes in a light–driven reaction and hydrolysis–photodecarboxylation cascade reactions is already reported,^{17,27,32,33} the present work demonstrates the possibility of applying a remarkable light source in an effective and innovative reactional system (Fig. 1).

Recently, Samire, Müller and co-workers reported that *CvFAP* is capable of C2–C12 decarboxylation, despite previous reports, by adjusting the pH to slightly acidic conditions.³⁰ Although it is known that *CvFAP* is capable of photodecarboxylation of fatty acids, such as palmitic and oleic acids, this approach for linear octane formation is the first of its class. *CvFAP* has an optimum pH range for higher chain decarboxylation, right around 8.5. In this range smaller chain acids are not decarboxylated by the enzyme, but by adjusting the pH in which the whole cell is suspended to 6.0 the enzyme is now capable of decarboxylating smaller chains such as C9, as shown by Samire for a range of mid-chain acids (Fig. 2).³⁰

After the cascade hydrolysis–ozonolysis reaction, pelargonic and azelaic acids could be easily isolated and taken into the final step to evaluate its reactivities in the protocol proposed by Samire, Müller and co-workers.³⁰ By using UV light at 365 nm, 30% organic phase (containing the acid) and 70% aqueous phase (containing the whole cell at pH 6.0), we could produce *n*-octane from pelargonic acid, with < 99% conversion and < 99% selectivity in under 30 min of residence time in triplicate (Scheme 3) (see the chromatographic profile: Fig. S24 in the ESI†). For azelaic acid, unfortunately conversions were not observed under the conditions studied and further reaction engineering and process optimization will be needed for applying such a starting material. *n*-octane provides a greater rating for fuel utilized in cars. The higher the better and more expensive. Varying from regular the lowest octane level, to midgrade and then premium, 91–94% octane.³⁴ This new approach rounds out the green, new approach for bio-fuel descendants from vegetal oil, a great source of renewable energy to the petrol industry. By hydrolysis, ozonolysis and

decarboxylation we converted CO₂ captured from the plants to vegetal oil to biofuel.

4. Conclusion

This study successfully demonstrates an integrated chemo-enzymatic cascade for converting canola oil into hydrocarbon fuels, highlighting significant advancements in process efficiency and sustainability. Through the combination of enzymatic hydrolysis, hydrogenation or ozonolysis, under continuous-flow conditions, photodecarboxylation conversion rates exceeding 90% were achieved, emphasizing the scalability and robustness of the proposed methodology.

The implementation of ultrasound-assisted continuous-flow hydrolysis greatly enhanced mass transfer and reaction efficiency, while the use of *in situ* hydrogen generation and a hybrid batch-flow approach for ozonolysis minimized environmental impact. Additionally, the novel application of violet light for photodecarboxylation with *CvFAP* proved highly efficient for alkane production, achieving complete conversion in short reaction times.

Overall, this work underscores the potential of integrating biocatalysis with continuous-flow technology for sustainable fuel production. The results open new pathways for the valorization of vegetable oils, contributing to the advancement of green technologies for renewable energy. Future studies should prioritize optimizing enzyme stability, expanding the substrate scope, and assessing the techno-economic feasibility for industrial implementation.

Data availability

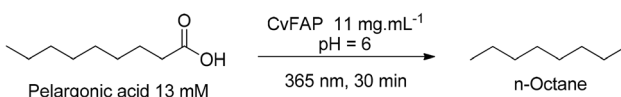
The data supporting this article have been included as part of the ESI.†

Conflicts of interest

There are no conflicts to declare.

Acknowledgements

The authors would like to express their gratitude to all institutions that made this work possible. We thank CAPES, CNPq, FAPERJ and Sinochem Brasil for financial support, and the São Paulo Research Foundation (FAPESP), Brasil, Process Number #2024/10284-0 (PRH 20.1 – ANP) for a research fellowship.



Scheme 3 Enzymatic photodecarboxylation transforms carboxylic acid into biofuel.



References

1 S. Shafiee and E. Topal, When will fossil fuel reserves be diminished?, *Energy Policy*, 2009, **37**(1), 181–189.

2 S. M. Ghazani and A. G. Marangoni, Healthy Fats and Oils, in *Encyclopedia of Food Grains*, Elsevier, 2016, pp. 257–267.

3 F. D. Gunstone, Production and Trade of Vegetable Oils, in *Vegetable Oils in Food Technology*, Wiley, 2011, pp. 1–24.

4 L. Maurice, H. Lander, T. Edwards and I. I. I. W. Harrison, Advanced aviation fuels: a look ahead via a historical perspective [Internet]. Available from: www.elsevier.com/locate/fuel.

5 J. Liu, E. Hu, W. Zheng, W. Zeng and Y. Chang, A new reduced reaction mechanism of the surrogate fuel for RP-3 kerosene, *Fuel*, 2023, **331**, 125781.

6 S. L. Douvartzides, N. D. Charisiou, K. N. Papageridis and M. A. Goula, Green diesel: Biomass feedstocks, production technologies, catalytic research, fuel properties and performance in compression ignition internal combustion engines, *Energies*, 2019, **12**(5), 809.

7 S. Khan, M. Fazly Abdul Patah and A. W. D. W. Mohd, Synergistic effect with and without Ni metal over ZSM-5/SAPO-11 catalyst in hydrodeoxygenation of palm oil, in *IOP Conference Series: Materials Science and Engineering*, Institute of Physics Publishing, 2020.

8 R. G. Pratiwi and K. Wantala, Hydro-conversion of palm oil via continuously pyrolytic catalysis to biofuels over oxide-based catalyst derived from waste blood clamshell: Effect of magnesium contents, *Mol. Catal.*, 2022, **523**, 111468.

9 N. A. Kabbashi, N. I. Mohammed, M. Z. Alam and M. E. S. Mirghani, Hydrolysis of Jatropha curcas oil for biodiesel synthesis using immobilized *Candida cylindracea* lipase, *J. Mol. Catal. B: Enzym.*, 2015, **116**, 95–100.

10 Z. Yang, W. Jin, X. Cheng, Z. Dong, M. Chang and X. Wang, Enzymatic enrichment of n-3 polyunsaturated fatty acid glycerides by selective hydrolysis, *Food Chem.*, 2021, **346**, 128743.

11 C. Su, H. C. Nguyen, M. L. Nguyen, P. T. Tran, F. Wang and Y. Guan, Liquid lipase-catalyzed hydrolysis of gac oil for fatty acid production: Optimization using response surface methodology, *Biotechnol. Prog.*, 2018, **34**(5), 1129–1136.

12 P. B. Subhedar and P. R. Gogate, Ultrasound assisted intensification of biodiesel production using enzymatic interesterification, *Ultrason. Sonochem.*, 2016, **29**, 67–75.

13 D. Ghosh, A. B. Vir, G. Garnier, A. F. Patti and J. Tanner, Continuous flow production of xylooligosaccharides by enzymatic hydrolysis, *Chem. Eng. Sci.*, 2021, **244**, 116789.

14 A. Zhu, W. Feng, Z. Li, S. Cheng, Q. Chen, D. Fan, *et al.*, Cleaner enzymatic production of biodiesel with easy separation procedures triggered by a biocompatible hydrophilic ionic liquid, *Green Chem.*, 2020, **22**(6), 1944–1951.

15 B. Casali, E. Brenna, F. Parmeggiani, F. Tentori and D. Tessaro, Multi-step chemo-enzymatic synthesis of azelaic and pelargonic acids from the soapstock of high-oleic sunflower oil refinement, *Green Chem.*, 2022, **24**(5), 2082–2093.

16 F. Hasan, A. A. Shah and A. Hameed, Industrial applications of microbial lipases, *Enzyme Microb. Technol.*, 2006, **39**(2), 235–251.

17 L. A. D. Benincá, A. S. França, G. C. Brêda, R. A. C. Leão, R. V. Almeida, F. Hollmann, *et al.*, Continuous-flow CvFAP photodecarboxylation of palmitic acid under environmentally friendly conditions, *Mol. Catal.*, 2022, **528**, 112569.

18 G. Brêda, A. França, K. de Oliveira, R. Almeida and R. de Souza, Exploring Strategic Approaches for CvFAP Photodecarboxylation through Violet Light Irradiation, *J. Braz. Chem. Soc.*, 2024, **35**(8), 1–5.

19 R. S. Atapalkar, P. R. Athawale, D. Srinivasa Reddy and A. A. Kulkarni, Scalable, sustainable and catalyst-free continuous flow ozonolysis of fatty acids, *Green Chem.*, 2021, **23**(6), 2391–2396.

20 G. Farkas, J. Madarász and J. Bakos, Asymmetric Hydrogenation in Continuous-Flow Conditions, in *Asymmetric Hydrogenation and Transfer Hydrogenation*, Wiley, 2021, pp. 307–337.

21 C. M. Pacheco, W. Lima, F. A. Lima, M. R. B. P. Gomez, I. G. da Silva, L. S. M. Miranda, *et al.*, Levoglucosanone as a starting material for cascade continuous-flow synthesis of (R)- γ -carboxy- γ -butyrolactone, *RSC Adv.*, 2024, **14**(47), 34611–34619.

22 P. J. Cossar, L. Hizartzidis, M. I. Simone, A. McCluskey and C. P. Gordon, The expanding utility of continuous flow hydrogenation, *Org. Biomol. Chem.*, 2015, **13**(26), 7119–7130.

23 X. Li, Y. Tu and X. Chen, Photoinduced Single-Electron Reduction of Alkenes, *Eur. J. Org. Chem.*, 2024, **27**(2), 1–6.

24 R. G. Ackman and R. D. Burgher, Employment of ethanol as a solvent in small scale catalytic hydrogenations of methyl esters, *J. Lipid Res.*, 1964, **5**(1), 130–132.

25 E. Faillace, V. Brunini-Bronzini de Caraffa, M. Mariani, L. Berti, J. Maury and S. Vincenti, Optimizing the First Step of the Biocatalytic Process for Green Leaf Volatiles Production: Lipase-Catalyzed Hydrolysis of Three Vegetable Oils, *Int. J. Mol. Sci.*, 2023, **24**(15), 12274.

26 M. Musik, M. Bartkowiak and E. Milchert, Advanced Methods for Hydroxylation of Vegetable Oils, Unsaturated Fatty Acids and Their Alkyl Esters, *Coatings*, 2021, **12**(1), 13.

27 M. M. E. Huijbers, W. Zhang, F. Tonin and F. Hollmann, Lichtgetriebene enzymatische Decarboxylierung von Fettsäuren, *Angew. Chem.*, 2018, **130**(41), 13836–13839.

28 D. M. Freire, E. M. F. Teles, E. P. S. Bon and G. L. Sant'Anna, Lipase Production by *Penicillium restrictum* in a Bench-Scale Fermenter, in *Biotechnology for Fuels and Chemicals*, Humana Press, Totowa, NJ, 1997, pp. 409–421.

29 M. M. E. Huijbers, W. Zhang, F. Tonin and F. Hollmann, Light-Driven Enzymatic Decarboxylation of Fatty Acids, *Angew. Chem., Int. Ed.*, 2018, **57**(41), 13648–13651.

30 P. P. Samire, B. Zhuang, B. Légeret, Á. Baca-Porcel, G. Peltier, D. Sorigué, *et al.*, Autocatalytic effect boosts the production of medium-chain hydrocarbons by fatty acid photodecarboxylase, 2023.



31 J. Bassut, Â. M. R. Rocha, S. da, A. França, R. A. C. Leão, C. M. F. T. Monteiro, C. A. M. Afonso, *et al.*, PEG600-carboxylates as acylating agents for the continuous enzymatic kinetic resolution of alcohols and amines, *Mol. Catal.*, 2018, **459**, 89–96.

32 Y. Ma, X. Zhang, W. Zhang, P. Li, Y. Li, F. Hollmann, *et al.*, Photoenzymatic Production of Next Generation Biofuels from Natural Triglycerides Combining a Hydrolase and a Photodecarboxylase, *ChemPhotoChem*, 2020, **4**(1), 39–44.

33 A. S. França, G. C. Breda, K. T. De Oliveira, R. V. Almeida, F. Hollmann and R. O. M. A. De Souza, Impact of sunlight irradiation on CvFAP photodecarboxylation, *Front. Catal.*, 2023, **3**, 1165079.

34 U.S. Energy Information Administration, *Gasoline Explained*, 2022.

